Expanding the toolbox for dating basaltic lava sequences: ^{40}Ar–^{39}Ar dating of silicic volcanic glass from interbeds.

Simone Cogliati[1*], Sarah Sherlock[1], Alison Halton[1], Alena Ebinghaus[2], Simon Kelley[3], David Jolley[2], and Tiffany Barry[4]

[1]Faculty of Science, Technology, Engineering and Mathematics, The Open University, Walton Hall, Milton Keynes, MK7 6AA, UK

[2]Department of Geology and Petroleum Geology, University of Aberdeen, Meston Building, Aberdeen, AB24 3UE, UK

[3]School of GeoSciences, University of Edinburgh, Grant Institute, The King's Buildings, James Hutton Road, Edinburgh, EH9 3FE, UK

[4]School of Geography, Geology and the Environment, University of Leicester, University Road, Leicester, LE1 7RH, UK

**Corresponding author (e-mail: simone.cogliati@open.ac.uk)*

ABSTRACT

^{40}Ar–^{39}Ar dating of glass shards from silicic tuffs of the Ellensburg Formation (NW, USA) interbedding basaltic lavas yielded accurate, precise, reproducible plateau and isochron ages that are within error at the 2σ level. The age-spectra have flat plateaus and the inverse isochrons have atmospheric $^{40}Ar/^{36}Ar$ at the 2σ level. Ages of 12.00 ± 0.24 Ma, 11.37 ± 0.15 Ma, 10.67 ± 0.21 Ma, 10.70 ± 0.18 Ma are consistent with the stratigraphy of four of the dated layers, the age of 10.77 ± 0.18 Ma for a fifth layer is at odds with the stratigraphy. This discrepancy arises due to the effect of glass alteration that induced K- and Ar-loss. There is no evidence of excess ^{40}Ar or ^{39}Ar recoil. The new ages indirectly constrain the timing of eruption of the lavas above and below the ash beds. This demonstrates that volcanic glass from interbeds can be used as an additional tool for indirectly dating basaltic lava sequences, that is independent of the lavas, and complementary to other materials. Considering the numerous studies in which volcanic glass failed to provide reliable ^{40}Ar–^{39}Ar ages, additional and supportive constraints are still needed to assess the validity of the ages from glass shards.

Timing and temporal evolution of basaltic lava sequences emplacement (e.g. large igneous provinces) have been investigated using many geochronological techniques (^{40}K–^{40}Ar, ^{40}Ar–^{39}Ar, U–Pb, magnetostratigraphy, palynology - Evernden and James, 1964; Jolley *et al.*, 2008; Jarboe *et al.*, 2008; Barry *et al.*, 2010; Burgess *et al.*, 2014). Particularly,^{40}K–^{40}Ar and ^{40}Ar–^{39}Ar methods have been extensively used to provide precise ages of lavas but only with limited success (e.g. Halton, 2011; Barry *et al.*, 2010; 2013). The low-K contents of the lavas (K_2O ≤ 1.5 Wt.%) and of the main phenocryst phase, plagioclase, (K_2O ~ 0.1%), and the ease with which groundmass weather and undergo alteration have hampered ^{40}Ar–^{39}Ar analyses (e.g. Marzoli *et al.*, 1999; Courtillot *et al.*, 2000; Barry *et al.*, 2010). Analysis of whole-rock, groundmass, single crystals or interstitial glass can produce ^{40}Ar–^{39}Ar ages which are unreliable, and when more than 1 phase is analysed from a sample the data can be inconsistent. This has been variably ascribed to plagioclase xenocrysts (Barry *et al.*, 2012), plagioclase sericitization (Verati and Jourdan, 2013), glass devitrification (Fleck *et al.*, 1977), deposition of secondary minerals from circulating fluids (e.g. clays, sericite, zeolites - Verati and Jourdan, 2013), ^{39}Ar and ^{37}Ar recoil (Koppers *et al.*, 2000; Jourdan *et al.*, 2007), excess ^{40}Ar ($^{40}Ar_E$: ^{40}Ar that is neither radiogenic or atmospheric and has become decoupled from parent K) (Kelley, 2002) and K-loss and ^{40}Ar loss from mineral structures caused by the circulation of high-temperature fluids (McDougall and Harrison, 1999).

Due to the difficulty in obtaining precise ^{40}Ar–^{39}Ar ages from lavas, indirect methods of dating basaltic sequences have been used. For example, K-rich minerals in silicic tuffs interlayering lavas has been demonstrated to produce consistent, precise, and accurate, indirect, ^{40}Ar–^{39}Ar ages for basalts eruption (Henry *et al.*, 2006, 2017; Mahood and Benson, 2017). However, even alkali feldspars can sometimes yield older than expected ^{40}Ar–^{39}Ar ages due to their possible xenocrystic or detrital origin (e.g. Renne *et al.*, 2012) or presence of $^{40}Ar_E$ (e.g. Kelley, 2002). In such cases, in addition to ^{40}Ar–^{39}Ar dating of basalts, other independent geochronological tools and supportive constraints (e.g. stratigraphic position, pollen records or U–Pb ages of zircons from within the same interbeds) are still necessary to determine the timing of basalts emplacement and duration of quiescence periods between eruptions.

Taking into account that volcanic glass is the most abundant K-rich juvenile phase in silicic tuffs, glass samples from ash-rich interlayers can be potential candidates for producing indirect ^{40}Ar–^{39}Ar ages for basalt eruptions. Various volcanic glass types (ash shards, obsidian, pumice glass) have been tested for ^{40}K–^{40}Ar and ^{40}Ar–^{39}Ar dating of volcanic events

(Kaneoka, 1972; Drake *et al.*, 1980; Cerling *et al.*, 1985; Cheilletz *et al.*, 1992; Bigazzi *et al.*, 2005, 2008; Vogel *et al.*, 2006; McGarvie *et al.*, 2007; Morgan *et al.*, 2009; Clay *et al.*, 2011, 2015; Nyland *et al.*, 2013; Flude *et al.*, 2018; Moles *et al.*, 2019; Cogliati, 2019). In most cases, volcanic glass yielded impossibly low, or high, ^{40}Ar–^{39}Ar ages, that becomes apparent when the glass ages are compared to the stratigraphy and/or to the ages of co-existing alkali feldspars (e.g. Cerling *et al.*, 1985; Morgan *et al.*, 2009; Clay *et al.*, 2011). Such discrepancies have been ascribed to: glass weathering, devitrification and hydration with mobilization and loss of K, and/or Ar (Kaneoka, 1972; Cerling *et al.*, 1985; Morgan *et al.*, 2009; Flude *et al.*, 2018), presence of $^{40}Ar_E$ from incomplete degassing of magmatic Ar (Clay *et al.*, 2011; Flude *et al.*, 2018), and kinetic mass fractionation of Ar isotopes with sub-atmospheric $^{40}Ar/^{36}Ar$ ratios (e.g., Vogel *et al.*, 2006; Morgan *et al.*, 2009; Flude *et al.*, 2018). However, there has been some success through the use of fresh, unaltered glass (obsidians: Vogel *et al.*, 2006; McGarvie *et al.*, 2007; Morgan *et al.*, 2009) and glass shards (Nyland *et al.*, 2013; Moles *et al.*, 2019) where reliable ^{40}Ar–^{39}Ar ages matched existing constraints such as stratigraphy and/or ^{40}Ar–^{39}Ar ages of alkali feldspars.

Here, for the first time, we demonstrate that precise and accurate ^{40}Ar–^{39}Ar ages can be obtained from volcanic glass shards from silicic tuffs that are interbedding basaltic lavas. We provide an additional tool for indirectly dating the volcanism that is both independent of the lavas and complementary to other methods (U–Pb dating, magnetostratigraphy, palynology) and materials (e.g. K-bearing minerals, zircons). Thus, expanding the available toolbox for dating basaltic lava sequences.

We use glass shards from samples collected within interbeds of the Ellensburg Formation (Swanson *et al.*, 1979) providing new ^{40}Ar–^{39}Ar ages from the upper portion of the Columbia River Basalt Province (Reidel *at al.*, 2013). Due to the particular type of sample and the small size of the glass shards, it was not possible to determine the alteration of the glass a-priori in the field during collection. For this reason, the pristine nature of the glass is assessed by using a specific alteration index calculated from the results of electron microprobe analysis of glass shards and looking at the variability of the electron microprobe totals.

The validity and reliability of the method used to date glass shards is assessed by examining the Ar data, the shape of age spectra and inverse isochrons and their statistical fits as well as comparing the new ages with the stratigraphical position of the interlayers, relative positions of the upper and lower basalts and, where available, their ^{40}K–^{40}Ar and ^{40}Ar–^{39}Ar ages from previous studies. The use of stratigraphical constraints to assess the geological

significance of the ^{40}Ar–^{39}Ar ages from glass shards was possible only because clear field evidences show the position of the tuffs, from where the glass shards were derived, respect to the upper and lower basalt units.

The Ellensburg Formation

The Ellensburg Formation (Swanson *et al.*, 1979) groups together epiclastic and volcanoclastic sedimentary interbeds deposited in the central and western area of the Columbia River Basalt Province (Reidel *at al.*, 2013) between 15.6 Ma and 6.5 Ma (Swanson *et al.*, 1979). These deposits interlayer basaltic lavas of the Columbia River Basalt Group (CRBG) succession (Reidel *et al.*, 2013 and references therein) and mark hiatuses in the eruptive activity (Ebinghaus *et al.*, 2014 and references therein). Thickness and distribution of the sedimentary interbeds are controlled by the duration of volcanic hiatuses, the location of active eruptive centres, the local tectonic activity and the local topography (Ebinghaus *et al.*, 2014 and references therein). Several members of the Ellensburg Formation have been distinguished and divided according to their stratigraphic position, composition, sedimentary facies and relations with the upper and lower lava units (Ebinghaus *et al.*, 2014 and references therein). Volcanic facies comprise primary pyroclastic deposits, reworked volcaniclastic deposits and agglutinates (Ebinghaus *et al.*, 2014). Primary pyroclastic deposits are ash-fall layers erupted during the Cascade Range and Yellowstone activity and deposited on exposed CRBG lavas (Smith, 1988; Ebinghaus *et al.*, 2014, 2015); reworked volcaniclastic deposits comprise a mixture of ash shards, pumices, quartz, feldspars and lithic fragments derived from syn-eruptive pyroclasts reworked and re-sedimentated in fluvial and lacustrine environments (Swanson *et al.*, 1979; Smith, 1988; Ebinghaus *et al.*, 2014); agglutinates are basaltic bombs and blocks deposited proximal to the vent or transported and redeposited by fluvial currents not far from their original depocentre. All these deposits can be found in any member of the Ellensburg Formation, alone, or interbedding with sandstones, mudstones and clastic sediments.

Glass shards for ^{40}Ar–^{39}Ar dating are from samples collected in the Pasco Basin (Washington, U.S.) (Fig. 1a) from five volcanoclastic ash-rich lacustrine and fluvial interbeds from within the Selah and Rattlesnake Ridge Members of the Ellensburg Formation (Swanson *et al.*, 1979). These units are interlayered between Saddle Mountain Basalt lavas, near the

top of the CRBG succession (Fig. 1b). Detailed information on sample location, stratigraphic position and depositional environment are in supplementary file A1.

Sample characterization

The glass shards are from five compacted ash-rich siltstones that comprise volcanic glass shards, quartz, biotite, alkali-feldspars, amphibole, apatite, zircon and minor detrital components. Glass shards are alkaline to sub-alkaline rhyolites (Ebinghaus *et al.*, 2015) with K_2O content between 3.55 and 6.74 wt.%, electron microprobe totals between 90.53 and 97.40 wt.% and a Chemical Index of Alteration (CIA; Nesbitt and Young, 1982) between 53.83 and 65.14 (Table 1). MA-1-5M shows the maximum variability in term of K content, CIA and totals values, moreover it displays the highest CIA (average 59.09 ± 2.32, maximum value of 65.14) and the lowest totals (average 92.99 ± 1.45 Wt.%, minimum value 90.53 Wt. %). All the other samples have a mean CIA value of ~ 56 slightly outside the range of 45 - 55 given by Nesbitt and Young (1982) for fresh highly-alkaline rocks and mean totals of about 94 – 96 Wt. % (Table 1). Given the minimal variability of the CIA and electron microprobe totals mean values from one sample to another (CIA average range 56.5 – 59.0, totals average range 96 – 92, table 1), these parameters are not sufficient alone to predict the quality of the ^{40}Ar-^{39}Ar ages and additional criteria are necessary to assess the reliability of the ages. Details on electron microprobe analysis with a complete dataset are in supplementary file A2.

Analytical methods

The samples (e.g., Fig. 2A) were crushed and sieved (Fig. 2B - D) and the 63 μm size fraction (Fig. 2E) was cleaned ultrasonically with 2% HCl, acetone and deionized water (Fig. 2F). 20 - 40 mg of optically clean and transparent glass shards (Fig. 2F) were hand-picked, wrapped in aluminium foils, put in an Al cylindrical container together with biotite standard GA1550 (99.738 ± 0.104 Ma - Renne *et al.*, 2011) and irradiated, with Cd shielding, for 300 MWh (120 h) at the McMaster Nuclear Reactor (Canada).

Less than 20 mg of glass shards for each sample were step heated by using a SPI 1062 nm Nd-glass infra-red laser. Two Zr-Al SAES NP10k getters (one at room temperature, one at 440°C) and an inline cold nitrogen trap were used to purify gas sample prior admission to a MAP-215-50 noble gas mass spectrometer. Ion counts were detected using a secondary electron multiplier in peak-hopping mode with 5 minutes gettering time, 10 scan and 10

measurements for each Ar isotope. Data were corrected for blanks, ^{37}Ar and ^{39}Ar decay, atmospheric $^{40}Ar/^{36}Ar$ (298.56 – Lee *et al.*, 2006), mass discrimination (283 ± 2 for $^{40}Ar/^{36}Ar$) and neutron-induced interference reactions. The following correction factors, based on analyses of Ca and K salts, were applied: $(^{39}Ar/^{37}Ar)_{Ca}$ = 0.00065 ± 0.00000325, $(^{36}Ar/^{37}Ar)_{Ca}$ = 0.000265 ± 0.000001325, and $(^{40}Ar/^{39}Ar)_{K}$ = 0.0085 ± 0.0000425. A $^{40}K_{tot}$ decay constant of 5.5305 ± 0.0135E^{-10} (Renne *et al.*, 2011) was used for age calculation. Measurements of samples AR-1-6A and MA-1-5M were repeated to assess the analytical reproducibility and to test the reliability of the methods. For these two samples weighted mean ages are calculated. Full Ar isotopic data of blanks, samples and standard, data reduction software, J values and criteria for age calculation are in supplementary file A3.

In order to obtain more statistically valid inverse isochrons, ^{36}Ar values within error of 0 after blank correction, reported as negative in supplementary file A3, are ignored and $^{40}Ar/^{36}Ar$ ratios containing these values were not calculated and used to determine the isochron age. We also excluded those steps, at low or high temperature, that were not included in the plateau age calculations. This approach has enabled the direct comparison of the plateau and isochron ages. When plateau ages and isochron ages derived from the same samples were compared, those with MSWD closer to 1 were statistically preferred to represent the age of eruption of the sample. Where two ages with similar MSWD values were compared, the age with lower 2σ uncertainty was preferred over the other one. Unless otherwise stated, calculated ages are reported at the 2σ level.

Results

When plateau and isochron ages from the same sample are compared they are within error of one another at the 2σ confidence level (e.g., Fig. 3, 4 and 5). Where multiple aliquots are analysed the results were also reproducible (Fig. 4 and 5). Preferred ages of 12.00 ± 0.24 Ma (PRD-1-2A), 11.37 ± 0.15 Ma (AR-1-6A), 10.77 ± 0.18 Ma (MA-1-5M), 10.70 ± 0.18 Ma (SRD-1-2), 10.67 ± 0.21 Ma (BJ-1-10) follow selection criteria listed in the methods section. The ^{40}Ar–^{39}Ar ages have 1σ analytical uncertainties that are almost one order of magnitude more precise than those previously reported for whole-rock (± 0.7 - 0.2 Ma - 1σ) and plagioclase (± 0.4 - 0.1 Ma - 1σ) and in good agreement with the most precise ages obtained from lava groundmass (± 0.1 - 0.05 Ma - 1σ) (Barry *et al*., 2013).

All the age-spectra have flat plateaus (Fig. 3, 4 and 5). Rejected steps at the lowest release temperatures have negative or younger apparent ages with respect to the plateau likely caused by a possible ^{40}Ar-loss related to the alteration/hydration of small areas of the sample. Rejected steps at the highest release temperatures have older apparent ages likely caused by $^{40}Ar_E$ released from fluid inclusions within the glass. MA-1-5M has a highly disturbed age spectra with apparent ages that displays extremely variable 1σ analytical uncertainties (range: ± 0.07 - 3.15 Ma). This suggests possible disturbances of the Ar system most likely caused by some degrees of alteration of the glass. The flat shape of the age spectra for all the samples and the consistency of the obtained ages with the stratigraphic constraints and existing ^{40}Ar–^{39}Ar ages of upper and lower basalts for four of five samples (see discussion) suggest that ^{39}Ar recoil loss (Jourdan *et al.*, 2007) could, at most, have played only a minor role here.

All the inverse isochrons have ^{40}Ar/^{36}Ar ratios at atmospheric value (298.56; Lee *et al.*, 2006) when considered at the 2σ level (Fig. 3, 4 and 5). Some disturbances of the ^{40}Ar/^{36}Ar ratios for 3 out of 8 aliquots (208, MA-1-5M_1; 251, AR-1-6A_2; 253, AR-1-6A_3) (Fig. 4 and 5) could be related to minor hydration/alteration processes, which could be plausible given the CIA variations and low EMPA totals. However, another possible cause could be poor equilibration of the glass with atmosphere. Whichever process may be responsible, the effects, are minimal, given the concordance between plateau ages and isochron ages. In the inverse isochrons the lack of spread in ^{40}Ar:^{36}Ar:^{39}Ar and high proportion of radiogenic ^{40}Ar are responsible for the high 2σ uncertainties on the ^{40}Ar/^{36}Ar ratio of PRD-1-2A (± 190), AR-1-6A_1 (± 170), AR-1-6A_3 (± 140) and BJ-1-10 (± 120). Lower 2σ uncertainties on the ^{40}Ar/^{36}Ar ratio are detected for those isochrons with higher data dispersion such as for MA-1-5M_2 (± 82), AR-1-6A_2 (± 78) and SRD-1-2 (± 32). MA-1-5M_1 has a high 2σ uncertainty (± 120) associated to the Y-intercept even though it has a good data dispersion. This can be attributed to the elevated 1σ analytical uncertainty associated to each individual step.

Discussion

The new ^{40}Ar–^{39}Ar ages from very small (< 20 mg) amounts of clean glass shards isolated from ash-rich interbeds within the Ellensburg Formation are precise and reproducible. The minor differences in total gas isochron ages and plateau ages of different aliquots of MA-1-5M and AR-1-6A could be ascribed to the heterogeneous distribution of ^{40}Ar within the sample or

to the possible incorporation of altered glass in the aliquots. The plateau and inverse isochron ages agree within error and there is no evidence for any $^{40}Ar_E$ uptake or ^{39}Ar recoil beyond the 2σ error on the ages. These problems routinely affect the ^{40}Ar–^{39}Ar dating of glass but seem to be avoided in the glass shards here investigated. Although there is no clear evidence of Ar recoil loss from the samples, we suggest that testing with in-vacuum encapsulation methods could be used to confirm our data and to assess the effects of ^{39}Ar and ^{37}Ar recoil on glass shards.

Existing age and stratigraphic constraints indicate that: the ages of 12.00 ± 0.24 Ma (PRD-1-2A) and 11.34 ± 0.17 Ma (AR-1-6M) agree well with the stratigraphic position of these samples within the Selah Member between Umatilla (14.6 Ma ± n.a., Barry *et al.*, 2013) and Pomona Basalts (11.21 ± 0.42 Ma, Barry *et al.*, 2013) (Fig. 6). Similarly, the ages of 10.70 ± 0.18 Ma (SRD-1-2) and 10.67 ± 0.21 Ma (BJ-1-10) are also in good agreement with the stratigraphic position of these samples within the Rattlesnake Ridge Member, between the Pomona Basalt (11.21 ± 0.42 Ma, Barry *et al.*, 2013) and the Elephant Mountain Basalt (10.18 ± 1.02 Ma, Barry *et al.*, 2013) (Fig. 6). Our preferred weighted mean plateau age of 10.77 ± 0.18 Ma for MA-1-5M place the sample above Pomona Basalt in the Rattlesnake Ridge Member (Fig. 6). This is in contrast with direct field observations and with the stratigraphic position of the sample below Pomona Basalt in the Selah interbed (Fig. 1). This discrepancy suggests an erroneous young date most likely due to high degree of alteration of the glass during which K and Ar have been lost. This hypothesis seems plausible considering the higher than acceptable CIA values, the low EMPA totals and the highly disturbed age spectra.

Given the consistency of the glass ages with the stratigraphy and considering that the glass shards are not affected by $^{40}Ar_E$ and, aside from one sample, have not suffered of high degrees of alteration the following considerations can be made:

(1) The ages of 10.70 ± 0.18 Ma and 10.67 ± 0.21 Ma from ash layers between the Pomona and Elephant Mountain Basalts confirm a total duration of < 500 Ka years for the deposition of the Rattlesnake Ridge Member as previously proposed by Ebinghaus *et al.* (2015). However, because the age of 10.67 ± 0.21 Ma is from an ash layer from the middle portion of the interbed, the Elephant Mountain Basalt (10.18 ± 1.02 Ma - Barry *et al.*, 2013) could be younger than ~ 10.5 Ma and, thus, the interval between Elephant Mountain and Pomona Basalts could be much longer than 500 Ka.

(2) The ages of 11.34 ± 0.17 Ma and of 10.70 ± 0.18 Ma from two ash layers either side of the Pomona Basalt (11.21 ± 0.42 Ma, Barry *et al.*, 2013), suggest that the lavas could have been erupted within minimum period of ~ 0.29 Ma, between 11.17 Ma and 10.88 Ma.

(3) The ages of 10.70 ± 0.18 Ma and 10.67 ± 0.21 Ma are indistinguishable at the 1σ level and it is impossible to determine if they represent separate events. To improve the precision of the data it would be necessary to analyse bigger volume samples and even more multiple aliquots, however, this provides additional challenges in extracting enough clean batches of pure glass shards that are fundamental for obtaining good reliable ages. Multicollector mass-spectrometer (e.g. Argus, Nu-Noblesse - Mark *et al.*, 2009; Henry *et al.*, 2017) could also be used to return highly precise ^{40}Ar–^{39}Ar ages from glass shards. However, because of the analytical uncertainty inherent in detector cross-calibration, multicollector mass spectrometers could be of no advantage over the use of a single collector instrument when analysing small amount (20 mg) of fine-grained samples (63 μm). Further investigations are necessary on this point.

Conclusion

This study demonstrates that volcanic glass shards can be used to produce accurate, precise and reproducible ^{40}Ar–^{39}Ar ages for silicic tuffs interbedding basaltic lavas. We also provide an additional tool for dating the basaltic sequences indirectly. In obtaining such good results care is taken to characterize the shards and their selection is meticulous. High degrees of alteration only appear to have affected one sample that remains at odds with the stratigraphy, whilst all others are concordant with field constraints. At this level of precision, events closely spaced in time are indistinguishable without external constraints. More precise ^{40}Ar–^{39}Ar ages from glass shards can be used, in conjunction with other geochronological tools, to better constrain the age of eruption of basaltic lavas bracketing silicic tuffs interbeds.

Major conclusions on stratigraphy and geochronology of basaltic sequences and interbeds should ideally be based on data from more than one source and this attempt to improve and widen the application of glass shard dating provides an additional method that can be used even if, it may be a bit less precise than some alternatives. For these reasons, whilst our study has proven successful, we suggest that when glass shards are used as part of a study for dating basaltic sequences and interbeds other supportive constraints should be considered and these include: a pollen record within the same interbeds (Jolley *et al.*, 2008;

Ebinghaus *et al.*, 2015), ^{40}Ar–^{39}Ar ages from alkali feldspars (Henry *et al.*, 2006, 2017; Mahood and Benson, 2017) or U–Pb ages from zircons (Kasbohm and Schoene, 2018) in the same interbeds, ^{40}Ar–^{39}Ar ages from upper and lower lavas. Finally, where strong field evidences exist the stratigraphic position of the interbed from where the sample is derived and its relative position respect to upper and lower basalt units should also be taken into account.

Given that many studies on volcanic glass have yielded neither accurate nor precise ^{40}Ar–^{39}Ar ages, further work is required to establish the controls on the ^{40}K–^{40}Ar system. Understanding better the systematics of the ^{40}K–^{40}Ar system in volcanic glass is a beneficial goal to aim for, given its importance for obtaining reliable ^{40}Ar–^{39}Ar ages for silicic tuffs eruptions and, indirectly, for basaltic lavas for which there are silicic ash-bearing interbeds, or, for dating distal deposits or lake deposits where glass shards are the only available K-rich phase. The applications of these are particularly important for providing essential time constraints to establish links between volcanism and climate change (Moles *et al.*, 2019) and for dating paleontological and hominid finds bracketed by ash layers (Hall *et al.*, 1984).

ACKNOWLEDGEMENTS

This research has been funded by funded by The Open University Ar/Ar and noble gas laboratory. We thank James Malley for technical ^{40}Ar–^{39}Ar laboratory assistance. This research used electron microprobe data acquired by Dr. John Still at University of Aberdeen, Department of Geology and Petroleum Geology, School of Geosciences. We thank Stephen Self and an anonymous reviewer for comments on earlier drafts of the paper.

SUPPLEMENTARY FILE

A1: Samples location, stratigraphic position and depositional environments.

A2: Electron microprobe information with calibration and sample data.

A3: Ar isotopic data of blanks and samples, data reduction software, J values, criteria for age calculation and images of age spectra and inverse isochrons.

REFERENCES CITED

Barry, T.L., Self, S., Kelley, S.P., Reidel, S., Hooper, P. & Widdowson, M. 2010. *New $^{40}Ar/^{39}Ar$ dating of the Grande Ronde lavas, Columbia River Basalts, USA: Implications*

for duration of flood basalt eruption episodes. Lithos, **118** (2-3), 213–222, doi:10.1016/j.lithos.2010.03.014.

Barry, T.L., Self, S., Kelley, S.P., Reidel, S., Hooper, P. & Widdowson, M. 2012. *Response to Baksi, A., 2012, "New $^{40}Ar/^{39}Ar$ dating of the Grande Ronde lavas, Columbia River Basalts, USA: Implications for duration of flood basalt eruption episodes" by Barry et al., 2010 – Discussion*. Lithos, **146–147**, 300–303.

Barry, T. L., Kelley, S.P., Reidel, S.P., Camp, V.E., Self, S., Jarboe, N.A., Duncan, R.A. & Renne., P.R. 2013. *Eruption chronology of the Columbia River Basalt Group*. Geological Society of America, Special Papers **2497** (2), 45–66, doi.org/10.1130/2013.2497(02).

Bigazzi, G., Laurenzi, M.A. & Viramonte, J.G. 2005. *The obsidian from Quiron (Salta Province, Argentina): a new reference glass for fission-track dating.* Radiation Measurements, **39**, 613–616.

Bigazzi, G., Laurenzi, M. A., Soligo, M. & Tuccimei, P. 2008. *Multi-method approach to dating glass: The case of Basiluzzo Islet (Aeolian archipelago, Italy).* Journal of Volcanology and Geothermal Research, **177** (1), 244–250, doi.org/10.1016/j.jvolgeores.2007.10.005.

Burgess, S.D., Bowring, S. & Shen, S. 2014. *High-precision timeline for Earth's most severe extinction.* Proceedings of the National Academy of Sciences, **111** (9), 3316-3321, doi.org/10.1073/pnas.1317692111.

Cerling, T.E., Brown F.H. & Bowman J.R. 1985. *Low-temperature alteration of volcanic glass: Hydration, Na, K, ^{18}O and Ar mobility.* Chemical Geology: Isotope Geoscience section, **52** (3-4), 281-293.

Cheilletz, A., Clark, A.H., Farrar, E., Arroyo Pauca, G., Pichavant, M. & Sandeman, H.A. 1992. *Volcano-stratigraphy and $^{40}Ar/^{39}Ar$ geochronology of the Macusani ignimbrite field: monitor of the Miocene geodynamic evolution of the Andes of southeast Peru.* Tectonophysics, **205** (1-3), 307-327.

Clay, P.L., Kelley, S.P., Sherlock, S.C. & Barry, T.L. 2011. *Partitioning of excess argon between alkali feldspars and glass in a volcanic system*, Chemical Geology, **289**, 12–30.

Clay, P.L., Busemann, H., Sherlock, S.C., Barry, T.L., Kelley, S.P., McGarvie, D.W. & 2015. *$^{40}Ar/^{39}Ar$ ages and residual volatile contents in degassed subaerial and subglacial glassy volcanic rocks from Iceland*. Chemical Geology, **403**, 99-110.

Cogliati, S. 2019. *Noble gas analysis of volcanic glass particles: a better understanding of volcano degassing and implications for Ar/Ar dating of eruptions.* Ph.D. thesis, The Open University, 332 p.

354 Courtillot, V., Gallet, Y. et al. 2000. *Cosmic markers, $^{40}Ar/^{39}Ar$ dating and paleomagnetism of*
355 *the KT sections in the Anjar Area of the Deccan large igneous province*. Earth and
356 Planetary Science Letters, **182**, 137–156.
357 Drake, R.E., Curtis, G.H., Cerling, T.E., Cerling, B.W. & Hampel, J. 1980. *KBS Tuff dating and*
358 *geochronology of tuffaceous sediments in the Koobi Fora and Shungura Formations,*
359 *East Africa*. Nature (London), **283**, 368-372.
360 Evernden, J.F. & James, G.T. 1964. *Potassium-argon dates and the Tertiary floras of North*
361 *America.* American Journal of Science, **262**, 945-974, doi:10.2475/ajs.262.8.945.
362 Fleck, R.J., Sutter, J.F. & Elliot, D.H. 1977. *Interpretation of discordant $^{40}Ar/^{39}Ar$ age spectra*
363 *of Mesozoic tholeiites from Antarctica*. Geochimica et Cosmochimica Acta, **41**, 15-32.
364 Ebinghaus, A., Hartley, A.J., Jolley, D.W., Hole, M., & Millett, J. 2014. *Lava-sediment*
365 *interaction and drainage-system development in a large igneous province, Washington*
366 *State, U.S.*. Journal of Sedimentary Research, **84**, 1041–1063, doi: 10.2110
367 /jsr.2014.85.
368 Ebinghaus, A., Jolley, D.W., & Hartley, A.J. 2015. *Extrinsic forcing of plant ecosystems in a*
369 *large igneous province: The Columbia River Flood Basalt Province, Washington state,*
370 *USA*. Geology, **43** (12), 1107–1110, doi.org/10.1130/G37276.1.
371 Flude, S., McGarvie, D.W., Burgess, R. & Tindle, A.G. 2010. *Rhyolites at Kerlingarfjöll,*
372 *Iceland: the evolution and lifespan of silicic central volcanoes*. Bulletin of Volcanology,
373 **72**, 523-538.
374 Flude, S., Tuffen, H. & Sherlock, S.C. 2018. *Spatially heterogeneous argon-isotope*
375 *systematics and apparent $^{40}Ar/^{39}Ar$ ages in perlitised obsidian*. Chemical Geology, **480**,
376 p. 44-57.
377 Hall, C.M., Walter, R.C., Westgate, J.A. & York, D. 1984. *Geochronology, stratigraphy and*
378 *geochemistry of Cindery Tuff in Pliocene hominid-bearing sediments of the Middle*
379 *Awash, Ethiopia*. Nature, **308**, 26-31, doi.org/10.1038/308026a0.
380 Halton, A.M. 2011. *Paleocene-Eocene Time-Stratigraphic Calibration in the North Atlantic*
381 *Igneous Province with Focus on the Faroes-Shetland Basin Area*, Ph.D. thesis, The
382 Open University, 331 p.
383 Henry, C.D., Castor, S.B., McIntosh, W.C., Heizler, M.T., Cuney, M., & Chemillac, R. 2006.
384 *Timing of oldest Steens Basalt magmatism from precise dating of silicic volcanic rocks,*
385 *McDermitt caldera and northwest Nevada volcanic field* [abs]: Eos (Transactions,
386 American Geophysical Union), Fall Meeting Supplement, **44C**, 8.

Henry, C.D., Castor, S.B., Starkel, W.A., Ellis, B.S., Wolff, J.A., Laravie, J.A., McIntosh, W.C., & Heizler, M.T. 2017. *Geology and evolution of the McDermitt caldera, northern Nevada and southeastern Oregon, western USA.* Geosphere, **13**(4), 1066–1112, doi.org/10.1130/GES01454.1.

Jarboe, N.A., Coe, R.S., Renne, P.R., Glen, J.M.G. & Mankinen, E.A. 2008. *Quickly erupted volcanic sections of the Steens Basalt, Columbia River Basalt Group: Secular variation, tectonic rotation, and the Steens Mountain reversal*. Geochemistry Geophysics Geosystems, **9**(11), 1-24, doi:10.1029/2008GC002067.

Jolley, D.W., Widdowson, M. & Self, S. 2008. *Volcanogenic nutrient fluxes and plant ecosystems in large igneous provinces: An example from the Columbia River Basalt Group.* Journal of the Geological Society, London, **165**, 955-966, doi.org/10.1144/0016-76492006-199.

Jourdan, F. & Renne, P.R. 2007. *Age calibration of the Fish Canyon sanidine $^{40}Ar/^{39}Ar$ dating standard using primary K-Ar standards.* Geochimica et Cosmochimica Acta, **71**, 387–402, doi:10.1016/j.gca.2006.09.002.

Jourdan, F., Matzel, J.P. & Renne, P.R. 2007. *^{39}Ar and ^{37}Ar recoil loss during neutron irradiation of sanidine and plagioclase*. Geochimica et Cosmochimica Acta, **71**, 2791–2808, doi.org/10.1016/J.GCA.2007.03.017.

Kaneoka I. 1972. *The effect of hydration on the K/Ar ages of volcanic rocks*. Earth and Planetary Science Letters, **14**, 216-220.

Kasbohm, J & Schoene, B. 2018. *Rapid eruption of the Columbia River flood basalt and correlation with the mid-Miocene climate optimum.* Sciences Advances, **4** (9), eaat8223, DOI: 10.1126/sciadv.aat8223.

Kelley, S. 2002. *Excess argon in K-Ar and Ar-Ar geochronology.* Chemical Geology, **188** (1-2), 1–22, doi.org/10.1016/S0009-2541(02)00064-5.

Koppers, A.A.P., Staudigel, H. & Wijbrans, J.R. 2000. *Dating crystalline groundmass separates of altered Cretaceous seamount basalts by the $^{40}Ar/^{39}Ar$ incremental heating technique*. Chemical Geology, **166** (1-2), 139-158, doi.org/10.1016/S0009-2541(99)00188-6.

Lee, J. Y., Marti, K., Severinghaus, J. P., Kawamura, K., Yoo, H. S., Lee, J. B. & Kim, J. S. 2006. *A redetermination of the isotopic abundances of atmospheric Ar.* Geochimica et Cosmochimica Acta, **70** (17), 4507–4512, doi.org/10.1016/j.gca.2006.06.1563.

Ludwig, K. 2003. *Isoplot/Ex3.00. The Geochronological Toolkit for Excel*. University of California Berkeley, Berkeley Geochronology Center, Special Publication, 1a.

Mahood, G.A. & Benson, T.R. 2017. *Using $^{40}Ar/^{39}Ar$ ages of intercalated silicic tuffs to date flood basalts*: *Precise ages for Steens Basalt Member of the Columbia River Basalt Group.* Earth and Planetary Science Letters, **459**, 340–351, doi.org/10.1016/j.epsl.2016.11.038.

Mark, D.F., Barfod, D., Stuart, F.M. & Imlach, J. 2009. *The ARGUS multicollector noble gas mass spectrometer: performance for $^{40}Ar/^{39}Ar$ geochronology*. Geochemistry, Geophysics, Geosystems, **10**, 1-9.

Marzoli, A., Renne, P.R., Piccirillo, E.M., Ernesto, M., Bellieni, G. & De Min, A. 1999. *Extensive 200-million-year-old continental flood basalts of the Central Atlantic Magmatic Province.* Science, **284**(5414), 616–618, doi.org/10.1126/science.284.5414.616

McDougall, I. & Harrison, T.M. (eds) 1999. *Geochronology and Thermochronology by the $^{40}Ar/^{39}Ar$ method*, 2nd edition, Oxford University Press, New York, 269 p.

McGarvie, D.W., Stevenson, J.A., Burgess, R., Tuffen, H. & Tindle, A. 2007. *Volcano–ice interactions at Prestahnúkur, Iceland: rhyolite eruption during the last interglacial–glacial transition*. Annals of Glaciology, **45**, 38–47.

Moles, J. D., McGarvie, D., Stevenson, J. A., Sherlock, S.C., Abbott, P.M., Jenner, F.E. & Halton, A.M. 2019. *Widespread tephra dispersal and ignimbrite emplacement from a subglacial volcano (Torfajökull, Iceland)*. Geology, **47** (6), 577–580, doi.org/10.1130/G46004.1.

Morgan, L.E., Renne, P.R., Taylor, R.E. & Wolde Gabriel, G. 2009. *Archaeological age constraints from extrusion ages of obsidian: Examples from the Middle Awash, Ethiopia.* Quaternary Geochronology, **4** (3), 193–203, doi.org/10.1016/j.quageo.2009.01.001

Nesbitt, H.W. & Young, G. M. 1982. *Early proterozoic climates and plate motions inferred from major element chemistry of lutites*. Nature, **299** (5885), 715-717, doi.org/10.1038/299715a0.

Nyland, R.E., Panter, K.S., Rocchi, S., Di Vincenzo, G., Del Carlo, P., Tiepolo, M., Field, B. & Gorsevski, P. 2013. *Volcanic activity and its link to glaciation cycles: Single-grain age and geochemistry of Early to Middle Miocene volcanic glass from ANDRILL AND-2A core, Antarctica.* Journal of Volcanology and Geothermal Research, **250**, 106-128.

Reidel, S.P., Camp, V.E., Tolan, T.L., & Martin, B.S. 2013. *The Columbia River flood basalt province: Stratigraphy, areal extent, volume, and physical volcanology*. Geological Society of America Special Papers, **497** (1), 1–43, doi.org/10.1130/2013.2497(01).

Renne, P.R., Balco, G., Ludwig, K.R., Mundil, R. & Min, K. 2011. *Response to the comment by W.H. Schwarz et al. on "Joint determination of ^{40}K decay constants and $^{40}Ar^*/^{40}K$ for the Fish Canyon sanidine standard, and improved accuracy for $^{40}Ar/^{39}Ar$ geochronology" by P.R. Renne et al. (2010).* Geochimica et Cosmochimica Acta, **75** (17), 5097–5100, doi.org/10.1016/j.gca.2011.06.021.

Renne, P.R., Mulcahy, S.R., Cassata, W.S., Morgan, L.E., Kelley, S.P., Hlusko, L.J. & Njau, J.K. 2012. *Retention of inherited Ar by Alkali Feldspar xenocrysts in a magma: Kinetic constraints from Ba zoning profiles.* Geochimica et Cosmochimica Acta, **93**, 129-142, doi: 10.1016/j.gca.2012.06.029.

Schwanethal, J., 2006. ArMaDiLo instruction Manual, 11.

Smith, G.A. 1988. *Sedimentology of proximal to distal volcaniclastics dispersed across an active foldbelt: Ellensburg Formation (late Miocene).* Central Washington. Sedimentology, **35** (6), 953-977, doi:10.1111/j.1365-3091.1988.tb01740.x.

Swanson, D.A., Wright, T.L., Hooper, P.R., & Bentley, R.D. 1979. *Revisions in Stratigraphic Nomenclature of the Columbia River Basalt Group: U.S.* Geological Survey Bulletin, **1457**, 59.

Verati, C. & Jourdan F. 2014. *Modelling Effect of Sericitization of Plagioclase on the 40K/40Ar and 40Ar/39Ar Chronometers: Implication for Dating Basaltic Rocks and Mineral Deposits.* Geological Society, London, Special Publications, **378** (1), 155-74, doi:10.1144/SP378.14.

Vogel, N., Nomade, S., Negash, A. & Renne, P.R. 2006. *Forensic $^{40}Ar/^{39}Ar$ dating: a provenance study of Middle Stone Age obsidian artifacts from Ethiopia.* Journal of Archaeological Science, **33** (12), 1749–1765, doi.org/10.1016/j.jas.2006.03.008.

York, D.1969. *Least squares fitting of a straight line with correlated errors*. Earth and Planetary Science Letters, **5**, 320–324, doi.org/10.1016/S0012-821X(68)80059-7.

TABLE

Table 1. *K_2O content, CIA and electron microprobe totals of the glass shards and plateau and isochron ages with relative ^{39}Ar* comprised within plateau, $^{40}Ar/^{36}Ar$ isochron intercepts and MSWD values*

Sample	K_2O*	CIA*	Totals*	Plateau age ± 2σ	MSWD	^{39}Ar*	Isochron age ± 2σ	MSWD	$^{40}Ar/^{36}Ar$	Weighted mean age ± 2σ
	Wt %		Wt %	(Ma)		(%)	(Ma)			(Ma)
BJ-1-10	5.66	55.07 - 57.44 (Av. 56.50)	93.66 - 94.84 (Av. 94.10)	**10.67 ± 0.21**	0.72	89.6	10.13 ± 0.92	0.53	317 ± 120	N.A
SRD-1-2	5.53	55.11 - 57.20 (Av. 56.28)	92.80 - 95.10 (Av. 94.09)	**10.70 ± 0.18**	0.99	100	10.65 ± 0.28	1.14	293 ± 32	N.A
PRD-1-2A	5.85	55.18 - 56.84 (Av. 56.12)	95.54 - 97.40 (Av. 96.37)	**12.00 ± 0.24**	0.31	75.4	11.86 ± 0.85	0.35	320 ± 190	N.A
MA-1-5M_1	5.25	56.10 - 65.14 (Av. 59.09)	90.53 - 96.34 (Av. 92.99)	10.42 ± 0.77	1.6	93.6	11.60 ± 3.70	1.7	208 ± 120	Age spectra **10.77 ± 0.18** MSWD = 0.88 Isochron 10.9 ± 1.2 MSWD = 0.17
MA-1-5M_2				10.79 ± 0.18	1.5	84.5	10.80 ± 1.30	1.9	294 ± 83	
AR-1-6A_1				11.64 ± 0.21	0.7	92.1	11.51 ± 0.47	0.85	326 ± 170	Age spectra 11.44 ± 0.44 MSWD = 3.0 Isochron **11.34 ± 0.17** MSWD = 0.36
AR-1-6A_2	5.22	53.83 - 57.79 (Av. 56.15)	95.11 - 96.23 (Av. 95.52)	11.30 ± 0.18	0.91	80.9	11.30 ± 0.21	0.91	251 ± 78	
AR-1-6A_3				11.42 ± 0.22	0.23	93.2	11.38 ± 0.37	0.19	253 ± 140	

Note: In bold preferred ages for the considered samples, selection criteria are listed in supplementary file A3. * Data are from electron microprobe analysis, the complete dataset is in supplementary file A2.

FIGURES

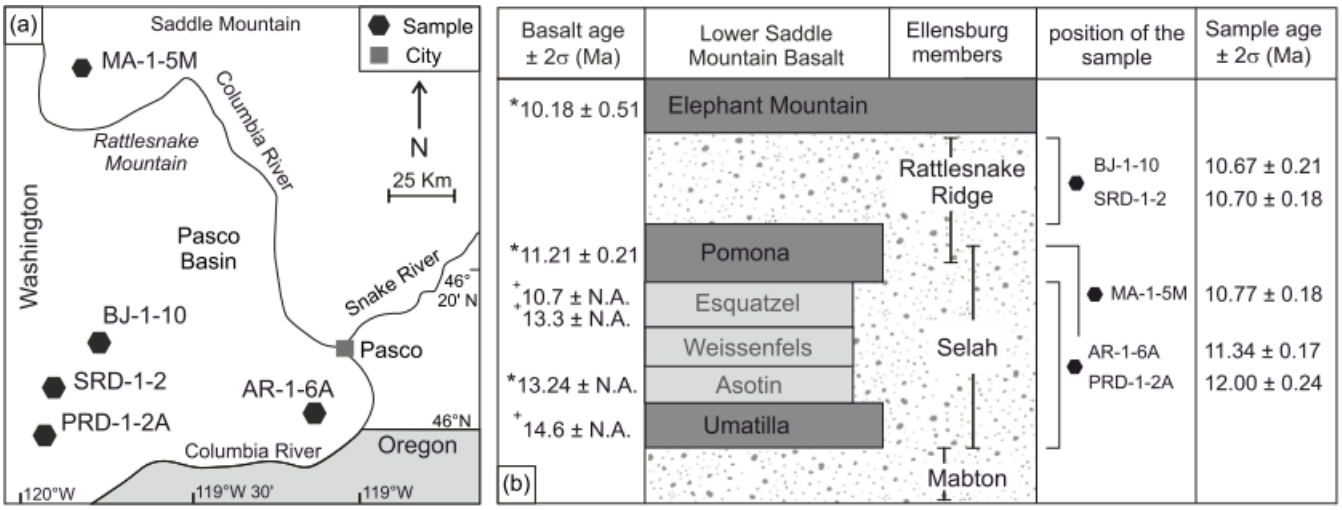

Figure 1. (a) Geographical map showing field locations of the samples analysed in this study (modified from Ebinghaus et al., 2014). **(b)** Stratigraphic positions and ages of the lower Saddle Mountain basalts (Reidel et al., 2013) and associated sedimentary interbeds of the Ellensburg Formation (Swanson et al., 1979; Ebinghaus et al., 2014). Black dots represent the position of the ash layers within the interbeds from where the glass shards were collected. Basalt ages are taken from Barry et al. (2013) while glass shards ages are from this study. * = Ar/Ar ages; $^{+}$ = K/Ar ages. All the age errors are quoted at the 2σ level; N.A.= age error not available.

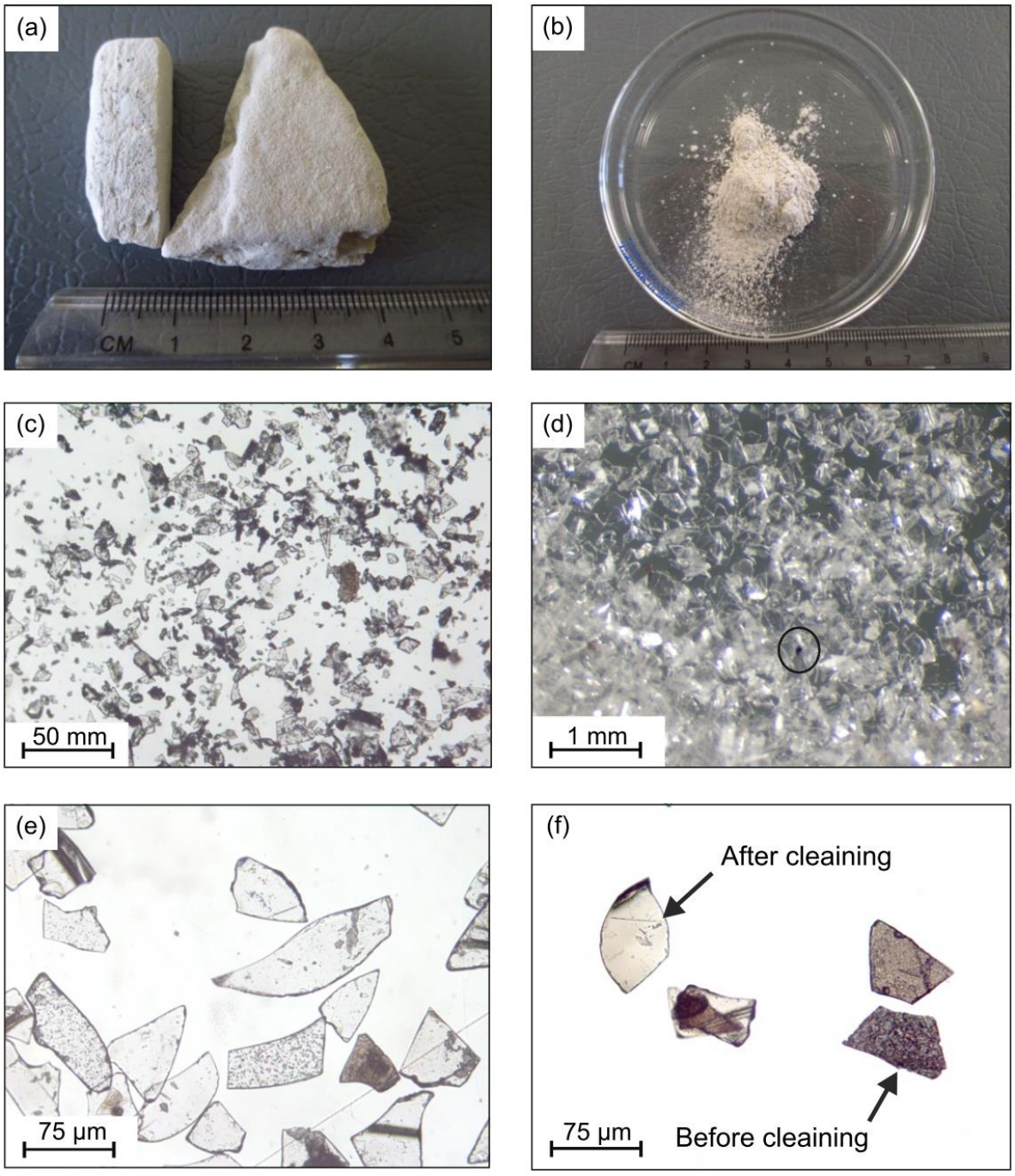

516

517 **Figure 2.** Sample preparation procedures: **(a)** Sample after collection and prior to processing – e.g. MA-1-6M. **(b)** Sample
518 ground using a ceramic mortar. **(c)** Transmitted light photograph under binocular microscope of glass shards of different
519 dimension after grinding and prior the sieving and cleaning stage. **(d)** Transmitted light photograph under binocular
520 microscope of glass shards of uniform size (63 µm) with extraneous dark materials (in the black circle). **(e)** Glass shards
521 remaining after the first pick selection. **(f)** Transmitted light photograph of sample MA-1-6M under binocular microscope. On
522 the right glass shards before acid cleaning. Visible small dark dots on shard surface represent some impurities or material
523 adhering to their surface. On the left clear and transparent glass shards after the cleaning stage ready for the analysis.

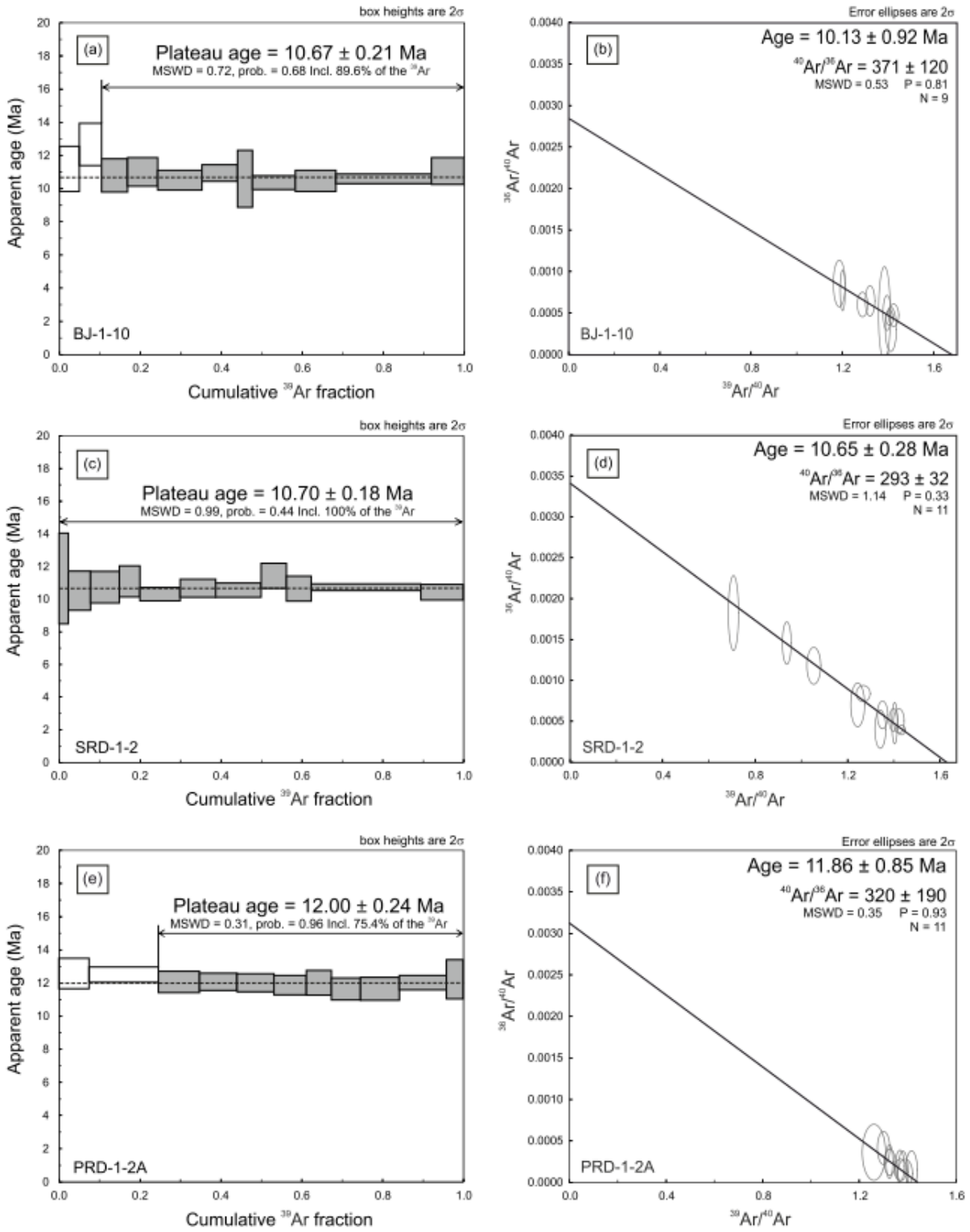

Figure 3. Age spectra and inverse isochrons for step heating experiments of samples BJ-1-10 **(a - b),** SRD-1-2 **(c- d)** and PRD-1-2A **(e- f)**. The age spectra have flat plateaus and the ages are closely aligned with isochron ages. All the ages are reported at the 2σ level.

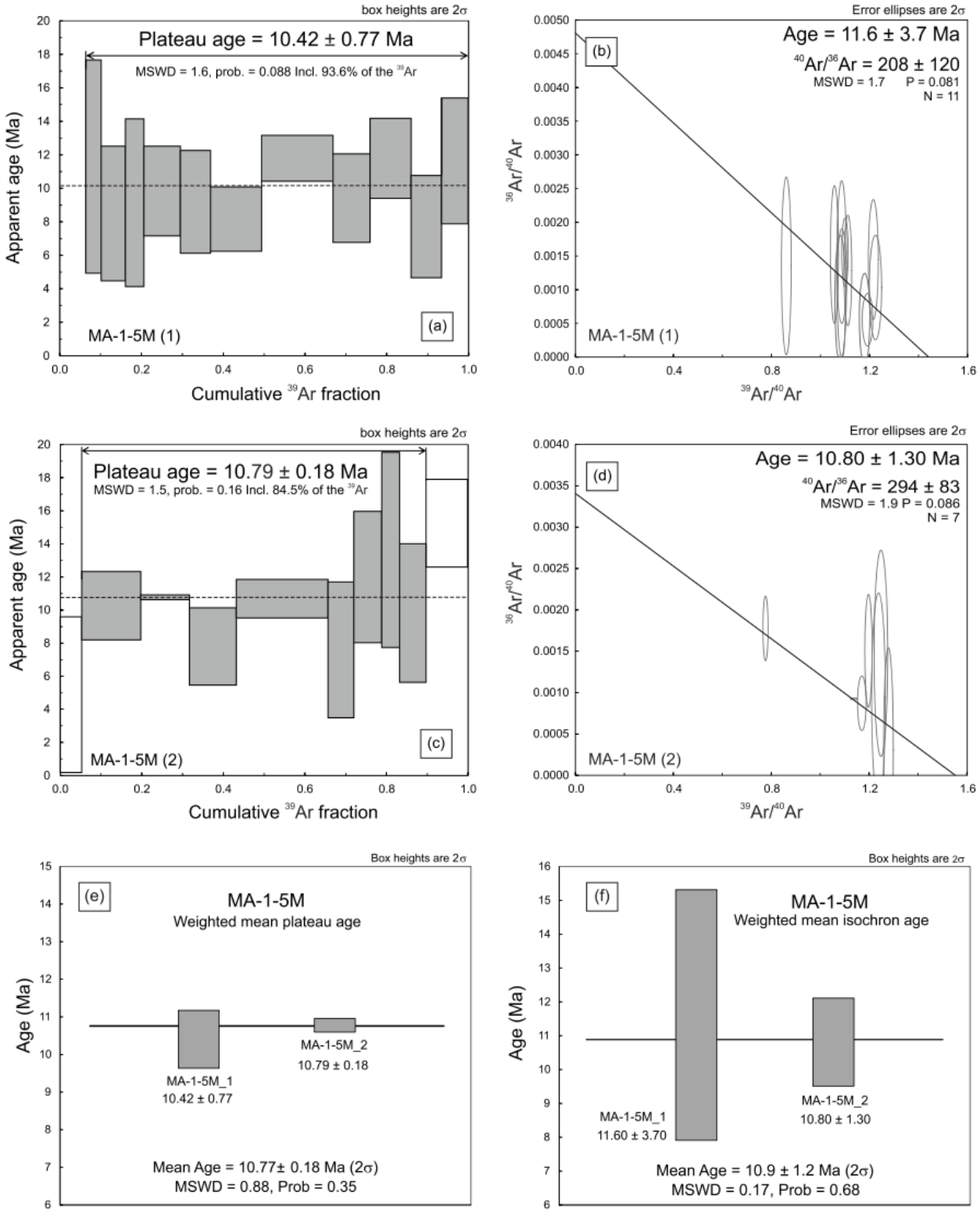

Figure 4. Age spectra and inverse isochrons for step heating experiments on two aliquots of sample MA-1-5M **(a - d)**; weighted mean plateau and isochron ages **(e – f)** for sample MA-1-5M. All the ages are reported at the 2σ level.

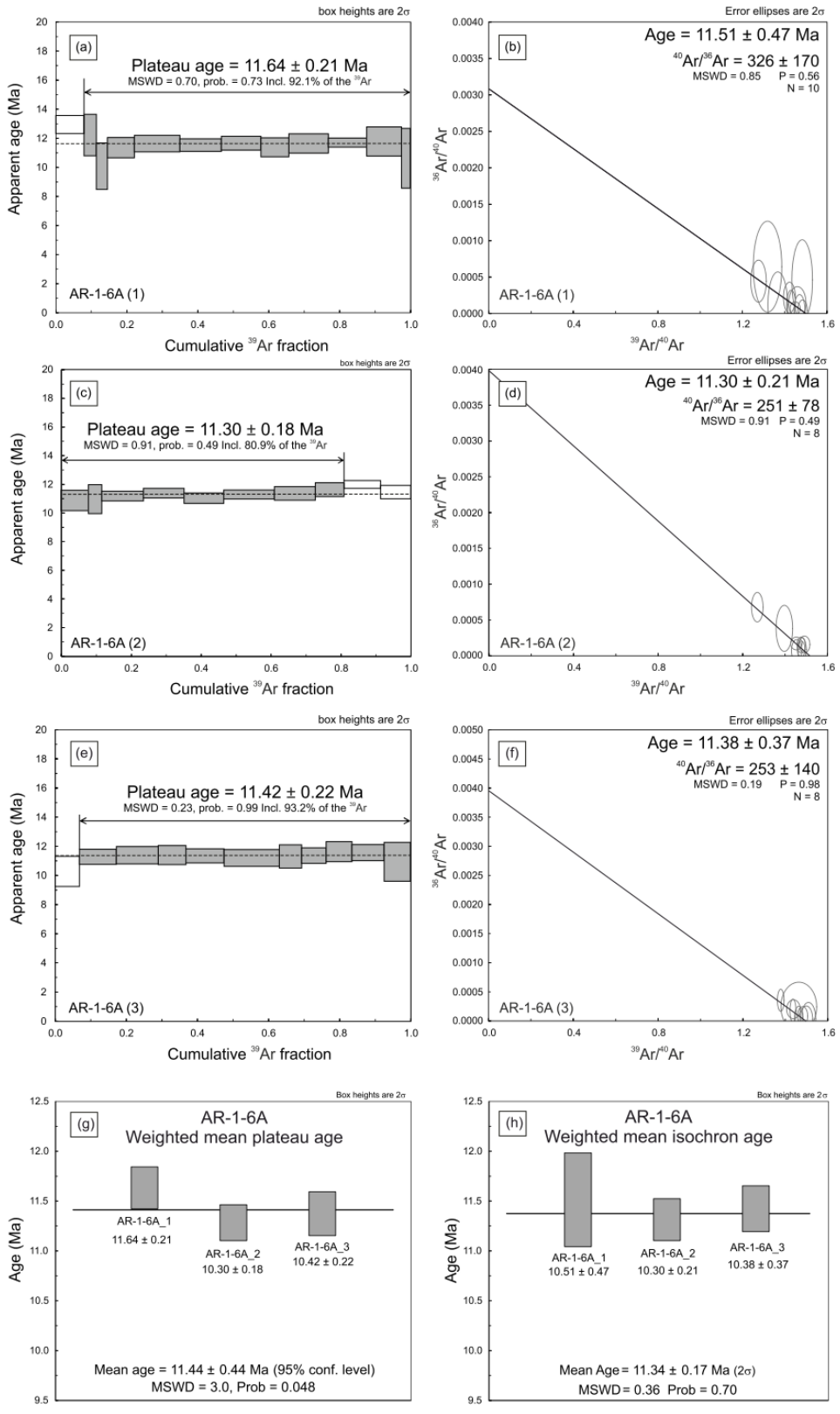

Figure 5. Age spectra and inverse isochrons for step heating experiments on three aliquots of sample AR-1-6A **(a - f)**; weighted mean plateau and isochron ages **(g – h)** for sample AR-1-6A. All the ages are reported at the 2σ level.

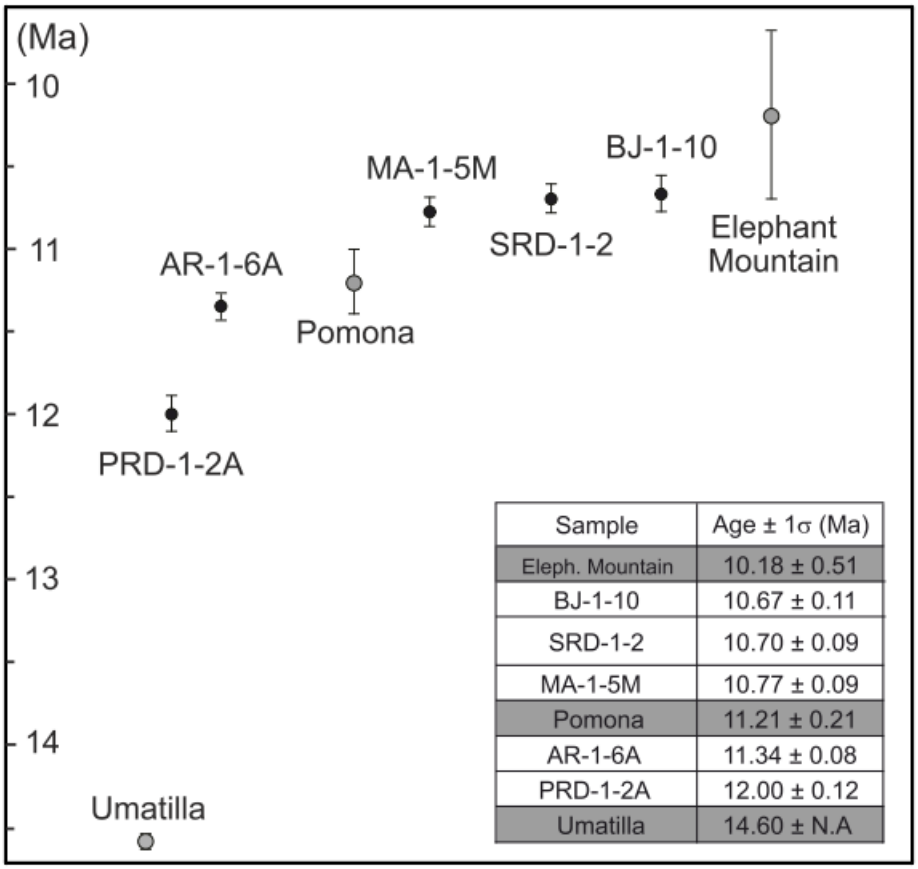

Sample	Age ± 1σ (Ma)
Eleph. Mountain	10.18 ± 0.51
BJ-1-10	10.67 ± 0.11
SRD-1-2	10.70 ± 0.09
MA-1-5M	10.77 ± 0.09
Pomona	11.21 ± 0.21
AR-1-6A	11.34 ± 0.08
PRD-1-2A	12.00 ± 0.12
Umatilla	14.60 ± N.A

Figure 6. Stratigraphic relationships between ages of the Umatilla, Pomona and Elephant Mountain Basalts (lower Saddle Mountain, CRBG) (grey dots) (Reidel et al., 2013) and ages of the ash layers investigated in this study (black dots). All the ages are quoted at the 1σ level. Basalt ages recalculated after the new age for the Fish Canyon Sanidine of Renne et al. (2011) – 28.294 ± 0.08 Ma – are indistinguishable from those calculated by Barry et al. (2013) with the value given by Jourdan and Renne (2007) of 28.03 ± 0.036 Ma. The age error for the Umatilla Basalt is not available and the error bar is only for illustrative scope.